Generic thermal cooling design for multicell converters

Jean-Christophe Crébier, André Andreta, Yvan Avenas, Yves Lembeye

Generic thermal cooling design for multicell converters

Jean Christophe Crebier, André Andreta, Yvan Avenas, Yves Lembeye
Univ. Grenoble Alpes, CNRS, Grenoble INP*, G2ELab, F-38000 Grenoble, France

Abstract

MulticCell Converters based on the implementation of numerous subsystems can be seen as arrays of conversion cells. These cells can be physically arranged in 1, 2 or 3 dimensions. This paper introduces a generic cooling design methodology to keep the temperature of the conversion cells below their maximum limits. Based on a set of characterization, the method can be applied to any converter array based on standardized conversion subsystems. A practical implementation based on PCB technology with forced air cooling technique is proposed as an illustration to highlight the considered approach. The methodology presented can be transferred to any multicell converter topology and/or cooling technologies.

1 Introduction

Interleaved, MultiCell power Converters (MCC) and Power Converter Arrays (PCA) are based on the association of similar and "standardized" power conversion subsystems, all sharing the same electrical constraints and producing, theoretically, the same losses [1-3]. On one hand, these converters offer several benefits such as higher apparent switching frequencies leading to higher efficiency and power density [4]. Additionally, multi-cell converters can satisfy numerous specifications with a limited set of components and subsystems, that can be implemented in a generic way. On the other hand, because many components are implemented, designers fear for control complexity, reliability issues but also costs, especially for low and medium voltage applications. To convince designers about the interest of MCC of PCA, topics such as thermal management, conducted and radiated EMI, robustness are also important topics to be addressed in order to maximize benchmark and comparison but also to guide in designing such converters. Especially, MCC and PCA are all based on standardized sub-systems, later called Conversion Standard Cells (CSCs). This strong feature is critical in terms of generic design and implementation, cost reduction and yield [5-6].

This paper investigates how the physical arrangement of multiples Conversion Standard Cells (CSCs) can be taken into consideration in order to derive a generic methodology for the thermal management design of MCC of PCA. Starting from an ideal and simplified case study, the paper describes how to manage physical implementations of parallel and series associations of conversion cells from the thermal point of view. Figure 1 shows the physical arrangement of an array on conversion cells, series and parallel arrangements are highlighted. The design and optimization of the cooling of these types of converters considers how the physical arrangement of CSCs affects the coolant flow ans the pressure drop over them.

Inspired from other applications where many cells are implemented in series and or in parallel such as in PV panels or in battery stacks [7], the paper investigates the methodology to implement the thermal management design in multi-cell converters. The first section introduces the main issues related to thermal management design of MCC and PCA converters and a methodology is proposed. The second section implements the approach based on a PCB based technology and a dedicated testing environment. Finally, the last section explores the effectiveness of the methodology and provides design guidance.

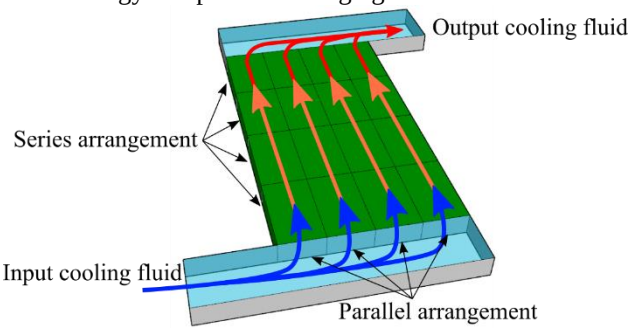

Figure 1. Schematic of a physical multi-cell converter arrangement together with its cooling path over the conversion cells.

2 Thermal management design of multicell converters

Power Converter Arrays and Multicell Converters are implemented with several standardized conversion sub-systems that needs to be cooled down. The thermal management can be carried out individually, at CSC level, paralleling cooling paths, as presented in figure 1. This is usually not a fully cost effective solution because it duplicates the cooling actuators and requires a careful design in order to avoid thermal coupling. On the other hand, implementing the cooling technique in series, as it is usually the case on PCB boards, requires extensive modelling and simulation to account for the strong thermal coupling conditions among the components and sub-systems that are cooled one after the other with the same coolant.

The next subsection investigates, for the specific case of standardized conversion cells (CSC), how the geometrical arrangement can be considered and how the cooling issue can be addressed. The methodology to optimize the thermal management design is also described. In all cases, this work focus on active cooling techniques, where the coolant

is flowing thanks to an actuator, a fan or a pump, depending on the fluid used for cooling.

2.1 Main issues in designing thermal cooling on multicell converters

Effective cooling management relies on two main issues. The first one is the temperature of the coolant. The second one is the value of the equivalent thermal resistance between the heat sources and the coolant. Knowing the losses and the maximum temperature rise allowed in the subsystem to be cooled down, the optimal thermal resistance can be derived with respect to coolant characteristics and temperature. Usually, the most critical thermal resistance in the heat propagation path is the interface between the subsystem exchange surface (e.g. the PCB or the heatsink) and the coolant (air, water, dielectric fluids…). It is usually characterized by an equivalent resistance that can be further characterized by a surface exchange and a heat transfer coefficient "h".

The main thermal propagation path for the heat, at subsystem level must be characterized or precisely modelled. If modelling techniques are today accurate, the most reliable approach to characterize the entire thermal propagation path remains the experimental characterization such as presented in [8].

The characterization procedure must consider the most critical operating points that will produce the largest amount of heat under the worst cooling conditions (low flow and high temperature fluid).

Once the elementary conversion cell thermal propagation path is characterized, it becomes possible to study the impact of parallel and series associations from the thermal point of view. An important assumption must be defined prior to analyse the associations. It is expected that the cooling fluid is entirely channelled to go through the CSCs in strictly the same manner (fluid velocity and flow regime) and without leakage. It is also expected that due to channelling, no significant edge impact occurs.

The physical series association of conversion cells on the path of the coolant (in this work, air flowing on PCBs) will produce coolant temperature rise from one cell to the other. This effect is illustrated in Figure 2. This temperature increase modifies the heat removal performances from one cell to the other. This effect must be taken into account in order to keep the last conversion cell below its maximum temperature, increasing the coolant flow to further reduce the conversion cell thermal resistance. Since the conversion cells are associated in series, from the thermal point of view, the pressure drop in the cells will sum up, introducing the need to increase the power of the coolant actuator accordingly.

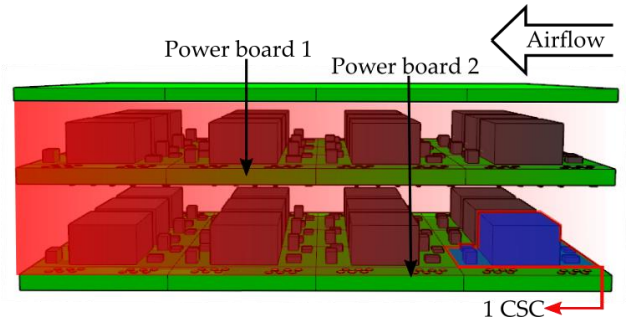

Figure 2. Qualitative picture of the impact of PCB based CSC series and parallel associations (4 rows, 3 columns, 2 boards/layers) on coolant temperature rise.

When conversion standard cells are physically associated in parallel, the coolant flow needs to be adapted accordingly in order to keep the heat transfer coefficient identical, no matter the number of cells associated in parallel.

Together with these issues, it is important to also keep in mind the impact of inlet and outlet of the coolant prior entering and going out of the CSCs physical arrangement.

2.2 Thermal design methodology

In order to analyse the thermal properties of the multi-cell converters, a complete experimental characterization must be carried out. Alternatively, Finite Element Modelling (FEM) and simulations can be carried out to extract important data. In table 1 is given the list of data set that must be acquired in order to set the models for the design.

Table I. Main parameter definition.

Parameter	Unit	Definition
Ta	°C	Coolant input temperature
Tmax	°C	CSC max temperature
T_X_{CSC}	°C	CSC number X Temperature
Afcsc	m^3/min	Air flowrate at CSC level
Afconv	m^3/min	Air flowrate at converter level
Pcsc	W	Power losses at CSC level
ΔPDcsc	Pa	Pressure drop at CSC level
ΔPDconv	Pa	Pressure drop at converter level
N_R		Number of rows (series arrang.)
N_C		Number of columns x layers (parallel arrangement)

At single CSC level, the "internal" temperature model T_{CSC} must be derived according to CSC losses P_{CSC}, ambient temperature Ta and coolant flow.

At PCA level, total pressure drop must be derived with respect to converter architecture (number of rows N_R, number of Columns x Layers N_C) and coolant flowrate.

In order to account for temperature rise in CSC physical series association ($N_R > 1$), another model is derived to express each CSC "internal temperature T_X_{CSC} with respect to ambient temperature Ta, P_{CSC}, coolant flow.

Once this is derived, the thermal design of any physical parallel and series association can be carried out. A simple algorithm is presented in Figure 3 in order to illustrate the methodology.

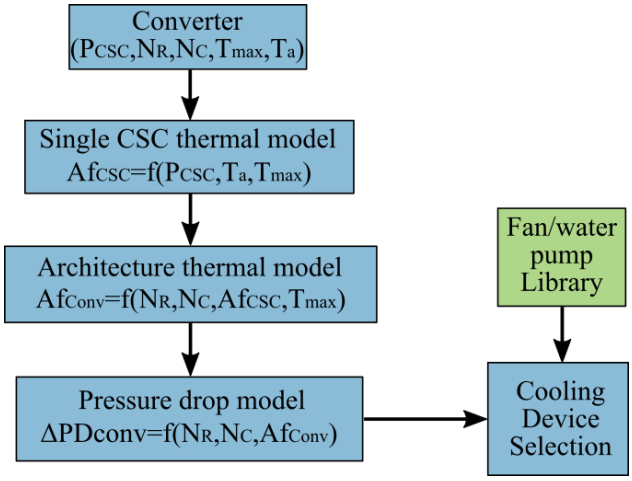

Figure 3. Thermal design methodology of physical parallel and/or series associations of CSCs.

3 Methodology practical implementation

In this section, the proposed methodology is applied to a practical case. PCA converters are designed and built from the series and parallel electrical and physical associations of conversion standard cells. The approach is presented in [9] and rises the opportunity to fulfil numerous specifications with the same sub-systems. The CSCs are low power low voltage (100W, 20V) autonomous, unity static gain, isolated DAB converters, designed and optimized based on a PCB technology. Their electrical association provides the opportunity to implement almost any transformation ratio, like a static transformer [10]. For any implementation, CSCs are physically arranged in rows, columns and boards before to be placed in a package/housing. N_R, N_C and N_L are respectively the number of rows, columns and boards. The thermal cooling parameters must be set according to these numbers in the most automated way.

The entire thermal design methodology is carried out from practical characterization based on a specific bench described in [8]. A picture of that bench is given Figure 4. It gives the opportunity to reproduce the packaging/housing of the PCA with, in addition the ability to tune air velocity and input temperature and to measure, output air temperature rise and pressure drop, air speed and fan power. Details about the measurement of pressure drop is presented in Figure 5. The two red dots highlighted in the figure indicates the positions in which the two probes of a differential manometer equipment are placed. At the output of the wind tunnel, an anemometer sensor is inserted in order to measure the air flowrate.

Figure 4. Left: Picture of a MCC under test inside the wind tunnel. Right: Fully instrumented characterization bench [PCIM].

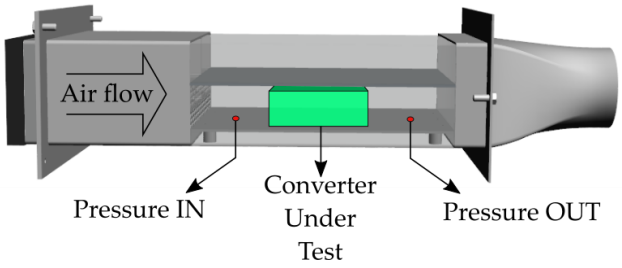

Figure 5. Lateral view of the wind tunnel with the physical locations of the pressure drop sensor.

The next three subsections describe the characterization and modelling processes in order to create the three models to be derived in the methodology presented in Figure 3. All experiments and the data extractions performed in this work are done using the characterization bench presented in Figure 4.

3.1 Single CSC Thermal model

The first model required in the thermal design process is responsible to define the required airflow to keep one CSC at a desired temperature with respect to the other parameters input temperature Ta, flowrate and power losses P. The thermal characterization of a CSC consists in performing experiments varying these three factors, one factor at time within the testing space described in Table II.

Table II. Characterization space for one CSC

Parameter	Unit	Range	Number of measure steps
Ambient Temp.	°C	25 to 65	10
Air flowrate	m^3/min	1.9 to 8	6
Power losses	W	1.3 to 10	15

Based on this Design of Experiment, the following curves and characteristics are derived. Figure 6 provides an illustration for these curves. There are several statistical modelling techniques capable of predicting the value of the converter temperature based on the experimental data. In this work, it was decided to use a parametrical model because it is easier to implement in the complete algorithm when compared to non-parametric models [11]. Three techniques were compared: Linear regression (LR), linear regression with interactions (LRI) and linear regression

pure quadratic (LRQ). The method that resulted the smallest Mean Squared Error was the LRQ. The selected model is represented by Equation (1) below.

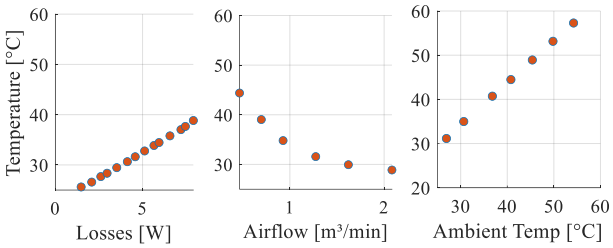

Figure 6. Experimental results of the CSC temperature versus the power losses, the air flowrate and the ambient temperature.

$$Temp_{CSC} = a1.T_{amb} + a2.Af_{CSC} + a3.P_{CSC} + b1.{T_{amb}}^2 + b2.{P_{CSC}}^2 + b3.{Af_{CSC}}^2 \quad (1)$$

3.2 Thermal model considering the architecture

As the air flows in the row direction, the air temperature increases in each conversion cell, as presented in Figure 2. In order to characterize this effect another experiment is performed. This second experimental setup consists in measuring the temperature in each row of the converter (5,1) at a fixed operating point and to evaluate the converter temperature for the corresponding row. The converter was submitted to four different setups, their details are presented in table III.

Table III. Experimental conditions.

Parameter	Unit	Setup I/III	Setup II/IV
Total input power	W	438	295
Efficiency	%	88.9	91.6
PCA total losses	W	48	25
Losses per CSC	W	9.6	5
Air flowrate	m^3/min	0.59/0.81	0.29/0.33
Ambient Temp.	°C	25	25

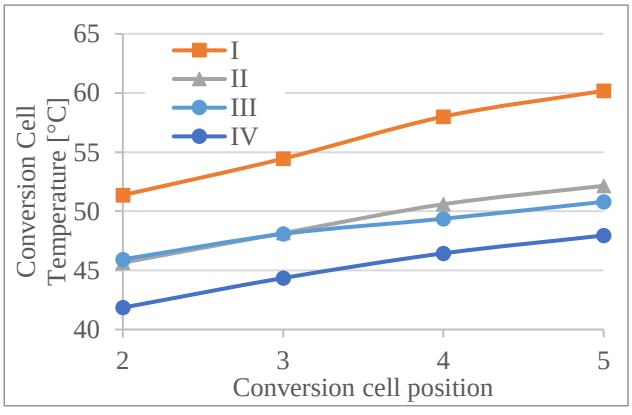

Figure 7. Temperature at the conversion cells versus the position of the conversion cell while the converter operates in four different operating points, presenting 48W and 25W power losses.

Similarly to the first model presented in section 3.1, a parametric model is derived using the experimental data. The model is presented in equation 2

$$Temp_{CSC} = k1.T_{amb} + \mathrm{k2}.Af_{CSC} + k3.N_R + k4.N_C \quad (2)$$

3.3 Pressure drop model

The airflow in the PCA is greatly impacted by the number of rows, columns and boards. As illustrated in Figure 1 and 2, extra numbers of columns and boards require more airflow to cool down the converter. On the other hand, extra rows add more obstacles to the air path, creating extra pressure drop. In order to understand and to represent these effects, a characterisation process with a few samples of PCA must be carried out. Figure 8 provides a picture of the realized and characterized prototypes. Their physical arrangement details are presented in table IV. These prototypes have been selected to characterize the elementary cell (1,1), a 1D column physical arrangement (1,5), a 1D row physical arrangement (5,1) and a typical 2D arrangement (3,4). With this set of prototype, a model can be derived according to the previous section. The characterisation setup is described in section 3 and presented in Figures 4 and 5.

Table IV: Arrangement, rated power and dimensions of the 4 prototypes.

PCA converter (rows, columns)	Rated Power (W)	Dimensions (WxLxH) [mm^3]
(1,1)	100	52 x 47 x 25
(5,1)	500	132 x 47 x 25
(1,5)	500	52 x 235 x 25
(3,4)	1200	112 x 141 x 25

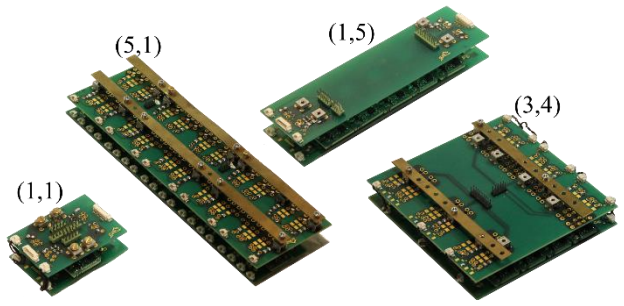

Figure 8. The four PCAs characterised in this work with their own numbers of rows and columns (N_R,N_C).

The 4 boards presented in Figure 8 were characterised inside the wind tunnel and data of their pressure drop and airflow were obtained. Figure 9 presents the experimental

curves obtained (curves with dots). Using this experimental data it is possible to fit an equation to predict the pressure drop at the converter with respect to the airflow and the architecture of the converter. Considering the curves described on Figure 9, a LRQ, similarly as fitted in section 3.1 has been implemented. The resulting general equation (3) is considered to derive any airflow and pressure drop with respect to PCA physical arrangements. Figure 9 presents the obtained experimental data (dots) and also the predictions of the model for various physical arrangements. As it can be seen, this model is satisfactory although, at low pressure drop, non-linear parts of experimental curves are not well represented by the model.

$$\begin{aligned} Pressure\ drop = {} & m1.lines + \mathrm{m2}.columns \\ & + \mathrm{m3}.Airflow \\ & + n1.lines^2 \\ & + n2.columns^2 \\ & + n3.Airflow^2 \end{aligned} \quad (3)$$

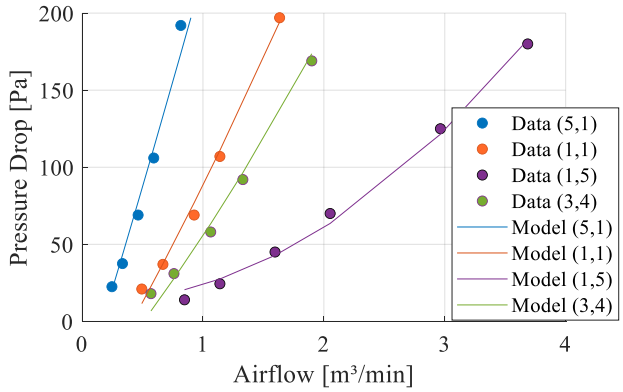

Figure 9. Airflow versus pressure drop chart. PCAs (5,1), (1,1), (3,4) and (1,5) obtained from practical characterisation data. PCAs (4,2), (4,4) and (1,4) characteristics are derived from the linear model equation (3).

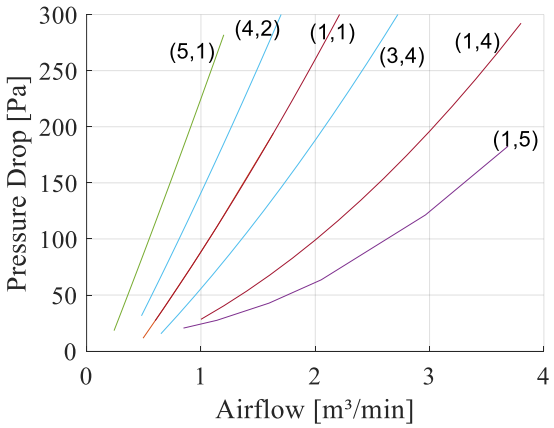

Figure 9. Predictions of the pressure drop versus the airflow for different architectures.

3.4 Thermal design process illustration

From these models, it is now possible to derive the coolant actuator device that would fit at best each PCA physical arrangement. This subsection presents, as an illustration, the thermal design process of a PCA having the characteristics listed in table V.

Table V. PCA main characteristics.

Factor	Unit	Value
Architecture	(N_R,N_C)	(4,2)
Operating Power	W	600
Efficiency	%	90
Total losses	W	60
Losses per CSC	W	7.5
Desired max temperature	°C	70
Ambient temperature	°C	30

The first step is to use equation (1) to find out the required airflow that is needed to keep a single CSC below the desired maximum temperature. Implementing all parameters in the model, a min Airflow level is derived and equal to:

$$Af_{CSC} = 0.58\ m3/min$$

Then, using equation (2), the impact of the Row arrangement, with N_R=4 in this example, is taken into account at first. In order to keep the temperature of the last CSC of each column below the desired limit, the airflow must be increased accordingly. The obtained value is equal to:

$$Af_{CSC} = 0.66\ m3/min$$

For the third step, the pressure drop model represented by equation (3) is used in order to derive the two critical parameters: the required airflow and resulting total pressure drop across the PCA. Since two columns are implemented in the selected PCA, the airflow must be twice the value obtained in the previous step. Looking at Figure 10, one can derive that the total pressure drop for a (4,2) PCA is estimated to:

$$\Delta P = 175\ Pa$$
$$Af_{Conv} = 1.32\ m3/min$$

From these two parameters, the coolant actuator can be defined. From a manufacturer database, the adequate fan device can be selected with respect to dimensions and mechanical power. A cross-check of the required airflow under estimated pressure drop on the manufacturer datasheet curve can be done in order to validate the selection. Some extra margin can be added to account for housing grid inlet and outlet protection if necessary. Considering a library of fans provided by *SanAce*, the fan model *9GA0612P6G001*, the fan operating point is checked as illustrated in Figure 10.

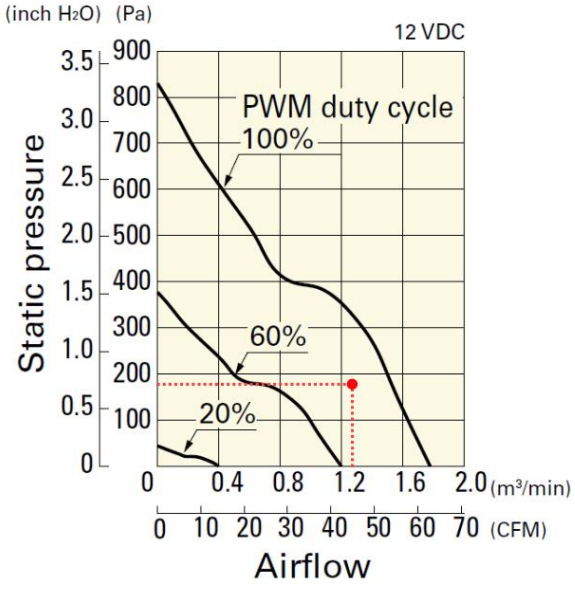

Figure 10. Operating point of the selected fan complying with calculated PCA necessary airflow and resulting pressure drop.

4 Comments

The models implemented in this paper were all first order models in order to ease comprehension. The model complexity can be refined as much as necessary in order to account for non linearity. Also, the impact of inlet and outlet where not considered although they may represent a significant contribution in the pressure drop. This should be considered in the full design. Finally, converter package airflow windows are usually secured with grid that may also contribute slightly to the pressure drop. It was not intended in this paper to take into account all additional contributors to the pressure drop and it is left to the reader to consider them.

Thanks to this methodology, the fan or pump needs are defined. Together with this selection, it is now possible to consider the impact of the cooling power consumption as well as the volume that represent the cooling actuator. In the illustration presented in the previous section, the fan is operated at 90% PWM for a power consumption of 16 W and its volume is 60 mm x60 mm x38 mm=0.1368 L. These data, integrated with the values for the PCA itself provides a more realistic estimate of the power density and the efficiency of the whole converter as illustrated in the table VI below.

Table VI. Inegration of Fan characteristics on Efficiency and power density of the whole converter.

	PCA alone	Fan	Whole converter (PCA + fan)
Power in	800	16	616
Losses (W)	80	16	72
Efficiency (%)	90		87.6
Volume (L)	0.338	0.136	0.474
Power density (kW/L)	2.36		1.69

Converter power density and efficiency are significantly affected by the introduction of the fan. Nonetheless, in this illustration, the losses level is quite high (10% of the transferred power). In addition, the max temperature at converter level is required to be kept quite low at 70°C, with a room temperature at 30°C, making more exigent its cooling needs.

5 Conclusion

This paper has introduced a generic thermal design methodology dedicated to MultiCell Converter and Power Converter Arrays. The methodology has been applied to a PCB based PCA converter design. It has been shown how is carried out the parameter extraction before deriving the main abacus. The method is effective and reliable. It is intended to ease thermal design of converters based on standardized conversion cells.

6 Literature

[1] M. Kasper, D. Bortis, G. Deboy, and J. W. Kolar, “Design of a Highly Efficient (97.7%) and Very Compact (2.2 kW/dm3) Isolated AC–DC Telecom Power Supply Module Based on the Multicell ISOP Converter Approach,” IEEE Trans. Power Electron., vol. 32, no. 10, pp. 7750–7769, Oct. 2017.

[2] M. Moosavi and H. A. Toliyat, “A Multicell Cascaded High-Frequency Link Inverter With Soft Switching and Isolation,” IEEE Trans. Ind. Electron., vol. 66, no. 4, pp. 2518–2528, Apr. 2019.

[3] A. G. Andreta et al., "A High Efficiency and Power Density, High Step-Up, Non-isolated DC-DC Converter Based on Multicell Approach," CIPS 2018;, Stuttgart, Germany, 2018, pp. 1-5.

[4] M. Kasper, D. Bortis, and J. W. Kolar, “Scaling and balancing of multi-cell converters,” in 2014 International Power Electronics Conference (IPEC-Hiroshima 2014 - ECCE ASIA), 2014, pp. 2079–2086.

[5] S. Sanchez, D. Risaletto, F. Richardeau and G. Gateau, "Comparison and design of InterCell transformer structures in fault-operation for parallel multicell converters," 2014 ECCE, Pittsburgh, PA, 2014, pp. 3089-3096.

[6] T. Lamorelle, S. Nguyen, J. C. Podvin, D. Rubio, Y. Lembeye and J. Crebier, "Multi-cell DC-DC converters - Input differential mode filtering generic design rules and implementation," PCIM Europe 2019, Germany, 2019, pp. 1-8.

[7] Wang, Tao, et al. "Thermal investigation of lithium-ion battery module with different cell arrangement structures and forced air-cooling strategies." Applied energy 134, pp. 229-238, .2014

[8] A. Andreta, A. Derbey, Y. Lembeye, F. L. Lavado Villa and J. Crebier, "Characterization Platform for Modular Power Converters," PCIM Europe 2018;, Nuremberg, Germany, 2018, pp. 1-6.

[9] A. G. Andreta, L. F. Lavado Villa, Y. Lembeye and J. Crebier, "Characterization and Modeling Technique of

Low Power Air-Cooled PEBB Modules," *2018 20th European Conference on Power Electronics and Applications (EPE'18 ECCE Europe)*, Riga, 2018, pp. P.1-P.9.

[10] J. Casarin, P. Ladoux and P. Lasserre, "10kV SiC MOSFETs versus 6.5kV Si-IGBTs for medium frequency transformer application in railway traction," *2015 International Conference on Electrical Systems for Aircraft, Railway, Ship Propulsion and Road Vehicles (ESARS)*, Aachen, 2015, pp. 1-6.

[11] G. James, D. Witten, T. Hastie, and R. Tibshirani, An Introduction to Statistical

Learning, vol. 103. New York, NY: Springer New York, 2013.